The Effect of the Artificial Backfill Materials on the Ampacity of the Underground Cables

Ossama E. Gouda[1], Adel Z. El Dein[2], and Ghada M. Amer[3]

[1]Faculty of Engineering, Cairo University, Giza Egypt
[2]High Institute of Energy, South Valley University, Aswan, Egypt
[3]High Institute of Technology, Benha University, Benha, Egypt

ABSTRACT

The backfill materials around under-ground power cables affect the maximum current carrying capacity of these cables. Usually backfill soils around under-ground power cables lose their moisture content, forming dry bands around the cables and leading to an increase in the thermal resistance and decreasing in maximum current carrying capacity. But according to the results of the experimental works which are carried out in this paper, it is noticed that some types of soil lost their moisture content faster than the other. This means that the dry band around the cable in some soils form faster than the others. The aim of this paper is to determine the best type of artificial soil that can be used as backfill material to minimize the effect of dry bands that cause thermal failure to the cable insulation.

Index Terms—Backfill Materials, Cable Ampacity, Dry band, Temperature Distribution

1. INTRODUCTION

The current rating of under-ground power cables is determined by the backfill soil thermal characteristics such as thermal resistivity of the soil, moisture content, suction tension of the soil and dry band formation. IEC 60-287 gives formulas to calculate the current ratings of under-ground power cables as a function of the cable properties and surrounding soil [1]. In this standard the soil thermal resistivity of the surrounding soil is supposed to be varies from 0.5 °C.m/w to 1.2 °C.m/w [3-5]. Under loading conditions of under-ground cables, the cable losses produce heat, which changes the moisture of the surrounding soil to vapor. The increase in vapor flow leads to temperature rise around the under-ground cables and formation of dry band [6-8]. In this paper natural and artificial nine samples of soil are investigated and tested for determination of their thermal properties. The aim of this paper is to obtain the most suitable backfill soil for the maximum current carrying capacity of under-ground power cables. Sand mixed with different ratios of lime as artificial backfill materials are tested. The data of XLPE distribution cables and backfill soils are used to calculate the maximum current carrying capacity and the temperature of the cable and backfill soils according to IEC 60287.

2. EXPERIMENTAL STUDY

2.1. Soil Samples under Testing

Nine types of natural and artificial soils are investigated and tested, for the determination of their properties. The classifications of the tested soils are given in Table 1.

Table 1.The Classification of the Investigated Samples

Sample number	Soil Sample	Weight percentage %				
		Gravel	Sand	Silt	Clay	Lime
1	Sand	1.5	88.5	10		
2	Lime	1.5	1.5	7		90
3	Clay	3	6	2	89	
4	Lime+Sand	0.5	48.5	2.5		48.5
5	Lime+Sand	0.3	24	1.7		74
6	Lime+Sand	1.4	74	0.6		24
7	Lime+Clay			2	24	74
8	Silt+Sand	10	60	30		
9	Clay+Salt+Sand	3	37	30	30	

2.2. Thermal Tests for Studying the Drying out phenomenon in soil Samples under Study

Fig. 1 shows a sketch for the arrangement used in this test. The sample under testing is contained in a cylinder of plastic material with a diameter of 100mm. The height of the soil sample is 100mm. In the top part, a heat flux (heat source) of known magnitude is introduced in a downward direction; this flux is measured by means of a calibrated heat flux meter. The bottom of the sample is in contact with a porous slab of sintered Pyrex glass with small pores (pores diameter is 5mm). This filter plate is glued on to a vessel of transparent plastic material, completely filled with water, a flexible tub connects the vessel with a leveling bottle, the water level in this bottle functions as an artificial ground water table. The cylinder containing the soil sample has been sealed off by an o-ring against the surrounding thermal insulation material. By this arrangement the moisture tension and thus water content can be adjusted. A number of thermo-couples is placed

978-1-4244-7534-6/10/$26.00 ©2010 IEEE

within the walls along the axis of the sample that provide a possibility of measuring the temperature distribution at different points in the soil sample [9].

3. RESULTS AND DISCUSSIONS

3.1. Dry and wet thermal Resistivities of the tested soil

The temperature distributions around the heat source, represent the cable losses for different tested soil samples, are recorded. The heat generated is controlled and changed by changing the current value. Fig. 2 gives the temperature versus distance for different tested soils when the tested soils are reached to steady state after 48 hours and pf=∞. As noticed in this figure there are two slopes for the distance-temperature relation ships.

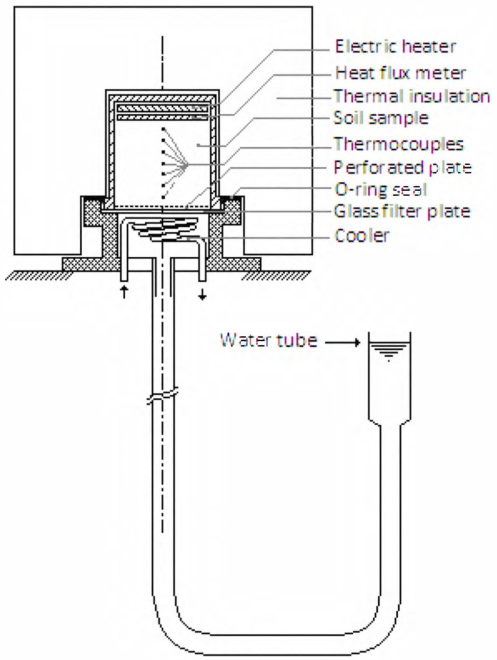

Figure 1 Arrangement used in drying out experiments.

The discontinuity of the curves indicates the separation between dry band and moist band. The slope of each band gives indication to the increase in the thermal resistivity that can be calculated for each test soil by the relation [10-16]:

$$\rho = \frac{\left(\frac{d\theta}{dZ}\right)}{Q_h} \qquad (1)$$

Where $\frac{d\theta}{dZ}$ is the temperature gradient °C/m,

ρ is the soil thermal resistivity °C.m/W and

Q_h is the heat flux density W/m^2

Table 2 gives the thermal resistivities of the tested soils when reaching to thermal steady state at pf=∞.

Table 2. Thermal resistivity of tested soils

Soil Type	ρ_{dry}	ρ_{wet}
Sand	2.036	0.96
Lime	2.35	0.941
Clay	1.568	0.627
50% Sand + 50% Lime	1.911	0.784
25% Sand + 75% Lime	2.156	0.822
75% Clay + 25% Lime	1.792	0.88
75% Sand + 25% Lime	1.304	0.522
Silt+Sand	1.9	0.756
Clay+Salt+Sand	1.65	0.83

The relation between percent lime in lime + sand mixture versus the time, which is required to form the dry band and the soil thermal resistivity, is given in Fig. 3. As shown in table 2 and in Figures 3 and 4 the soil mixture that contains 25% lime + 75% sand has the lowest soil thermal resistivity value for both dry and wet bands and has the longest time to form the dry band.

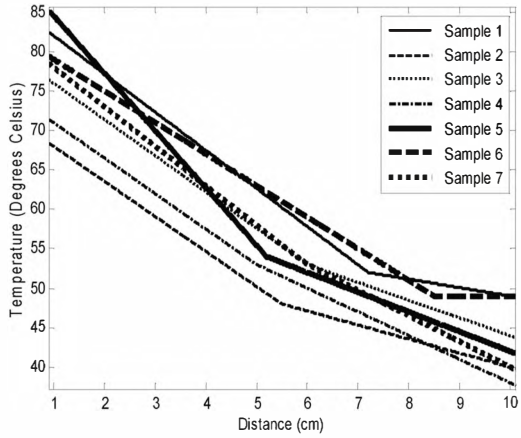

Figure 2: Temperature verses distance for different tested soils after 24 hours testing, with pf=∞, and Q_h=255w/m^2.

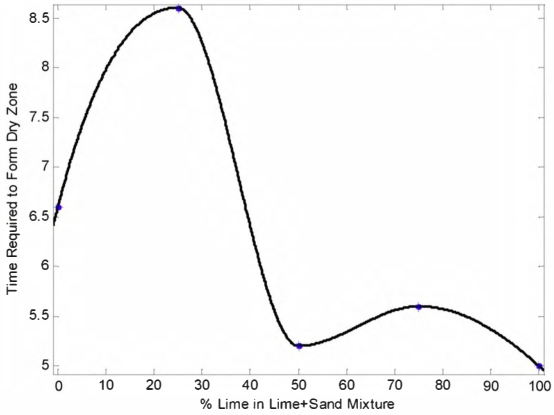

Figure 3. The relation between percent of Lime in Lime+Sand Mixture and time required to form dry band.

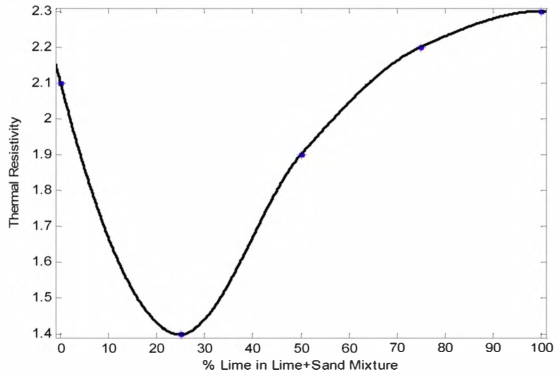

Figure 4. The relation between percent of Lime in Lime+Sand Mixture and thermal resistivity.

3.2. Effect of heat flux density on the time required to form the dry band

The heat flux density that represents the cable losses is changed to be 728 W/m^2, 468 W/m^2 and 344 W/m^2 and pf is kept constant at ∞. The time required to form the dry band versus heat flux density for sand, silt + sand and clay + sand is given in Fig. 5.

3.3. Effect of suction tension on the soil thermal resistivity

One important factor affecting the thermal soil resistivity and dry band formation around under-ground power cables is the suction tension. The moisture retention of soil is caused by capillarity. It is described by the moisture potential (α) which is defined as the suction tension of the soil in a water column. This quantity is usually expressed by the associated pf value which is defined by:

$$pf = \log(-100\alpha) \qquad (2)$$

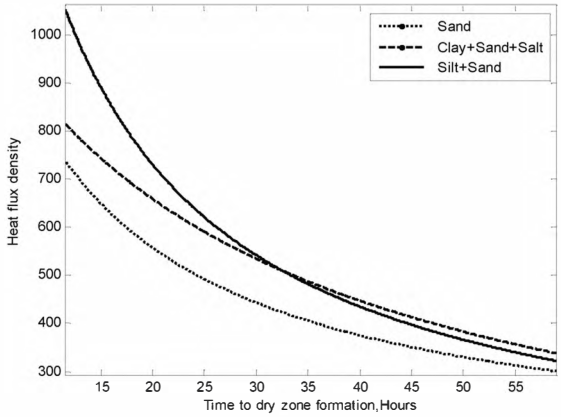

Figure 5. Time to steady state dry band formation versus heat flux density

Where; p_f returns the logarithm of base 10 of the suction tension. It is true that the suction tension depends on the moisture content, but it also depends more on the history of drying and wetting of the soil. In this paper, the thermal resistivities of the samples are tested at pf = 1, 2 and ∞ by changing the water column. The relation between soil thermal resistivities versus time is given in Figs. 6, 7 and 8 for sand, clay + sand and silt + sand, respectively. The thermal resistivities at steady stable in case of different values of suction tension for some of the tested soils are given in Table 3.

Table 3. Thermal soil resistivity for different tested soils and **pf**

Soil Type	Thermal Resistivities	pf		
		∞	2	1
Lime	ρ_{dry}	2.35	1.8	1.7
	ρ_{wet}	0.941	0.85	0.76
25% Lime +75% Sand	ρ_{dry}	1.304	1.22	1.02
	ρ_{wet}	0.522	0.50	0.48
Clay	ρ_{dry}	1.586	1.53	1.51
	ρ_{wet}	0.627	0.61	0.61
Sand	ρ_{dry}	2.03	1.7	1.46
	ρ_{wet}	0.968	0.75	0.75
Clay + Silt + sand	ρ_{dry}	1.65	1.6	1.469
	ρ_{wet}	0.83	0.756	0.705
Silt + Sand	ρ_{dry}	1.9	1.68	1.5
	ρ_{wet}	0.756	0.66	0.67

The findings in Table 3 are the more useful since they give reason to believe that the worst hydrological condition during dry season may be expressed in general as worst pf value in which the dry band has high thermal resistivity. For practical purpose this value may be taken independent of soil characteristics and density. When the water table is relatively high, its level determines directly the ambient pf value at the cable depth. In general the pf value in winter can be considered as 2 and less and in summer the pf value can be considered higher than 2. The results are useful in giving good figure about the winter and summer thermal resistivities of artificial and natural backfill soils.

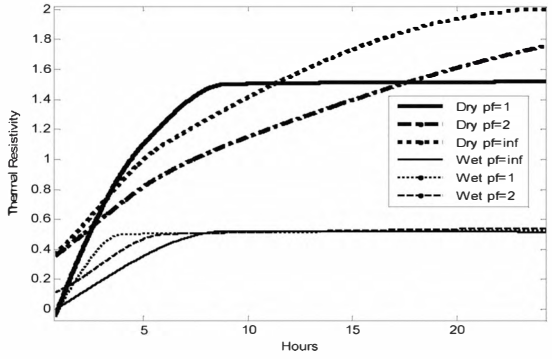

Figure 6. Soil thermal resistivity of sand as a function of time for different values of pf.

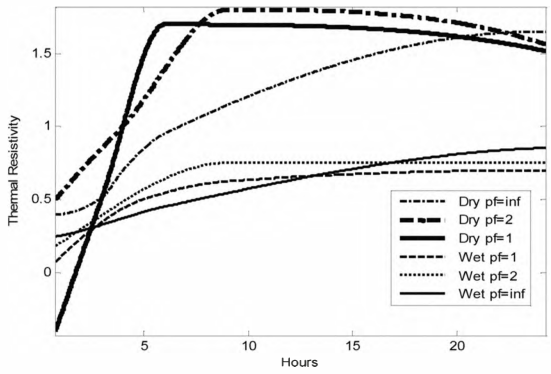

Figure 7. Soil Thermal resistivity of Clay+Silt+Sand as a function of time for different values of pf.

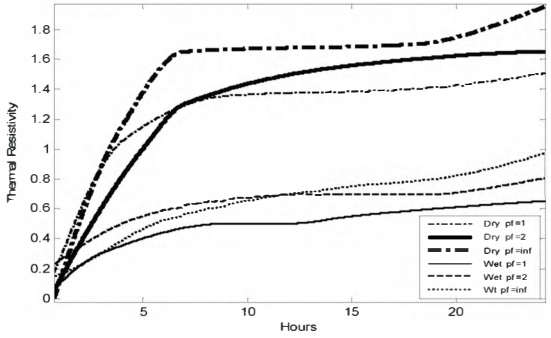

Figure 8. Soil thermal resistivity of silt + sand as a function of time for different values of pf.

3.4. Maximum current carrying capacity

The maximum current carrying capacity of a buried cable is calculated according to IEC 60287-1-3 taking into consideration the dry band formation around the under-ground cables [1]. Table 4 gives the ratio between the thermal resistivities (dry and moist bands) ν and the critical temperature θ_x, at which the dry band is formed, that for some tested soil and various pf. These values are used in the calculation of the under-ground power cable maximum current carrying capacity with dry band formation. Table 4 also gives the calculated under-ground power cable (11-kV and 33-kV) maximum current carrying capacity with and without dry band formation for some tested soil and various pf.

3.5. Temperature Distribution around Under-Ground Cable

Fig. 9 shows the geometry of a case study, which consists of three core cable (11-kV), which is directly buried in the soil at 0.8m depth. The cable is loaded by 352Amp; hence the maximum conductor temperature is fixed at 90°C. The cable construction details are given in Fig. 10.

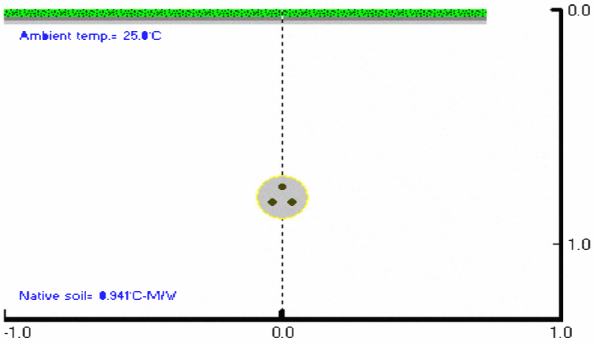

Figure 9. Geometry of case study

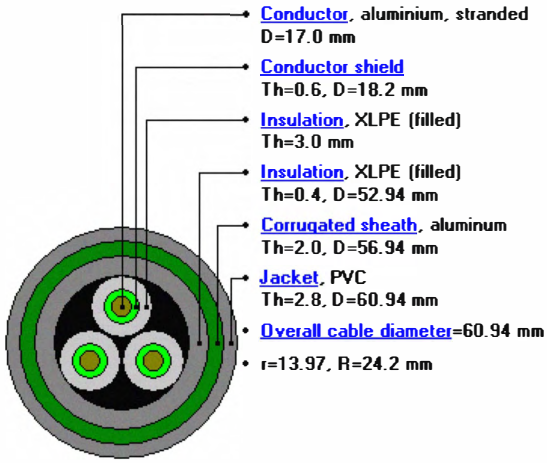

Figure 10. Construction details of the 11kV cable

In an under-ground cable system the main heat transfer mechanism is by conduction. Since the longitudinal dimension of a cable is always much larger than the depth of the installation, the problem becomes a two-dimensional heat conduction problem. The finite element method is used to study the temperature distribution around the under-ground cables. The thermal field in the cable medium is governed by the following differential equation [15-19]:

$$\frac{\partial}{\partial x}[k\frac{\partial \theta}{\partial x}]+\frac{\partial}{\partial y}[k\frac{\partial \theta}{\partial y}]=-q \qquad (3)$$

Where θ denotes the temperature at any point in xy plane around the under-ground cable, k represents the thermal conductivity and q is the heat generation per unit time and t denotes the time.

For any homogeneous region of a given thermal conductivity and heat generation rate, equation (3) can be solved for the temperature at any point (x,y) in the region subject to specified boundary conditions. The power cable thermal circuit includes various regions of complicated shapes having different values of thermal conductivities and heat generations. The finite element

method exploits the theory that the solution of equation (3), namely $\theta(x,y)$ is that which minimizes the following function:

$$F = \iint (\frac{1}{2}k[(\frac{\partial\theta}{\partial x})^2 + (\frac{\partial\theta}{\partial y})^2] - q\theta)dxdy \quad (4)$$

The cable medium is partitioned into small elements, normally triangles, forming a mesh as shown in Fig. 11. The minimization of equation (4) is performed over the finite element mesh yielding a set of linear equations of the form:

$$H\theta = b \quad (5)$$

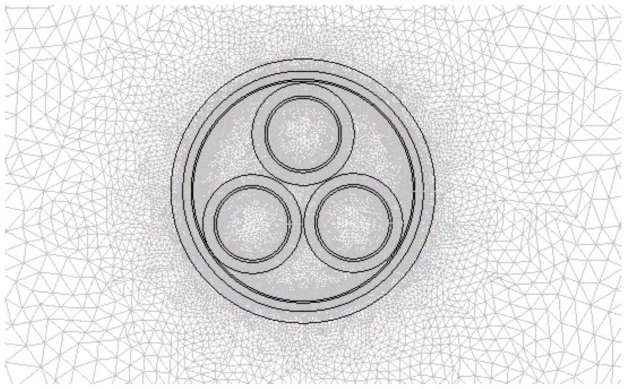

Figure 11. Sample of a finite element meshes

Table 4. The ratio of dry to wet thermal resistivities, critical temperature to form the dry band and Maximum Current Carrying Capacity for different soils under testing at Various **pf.**

Soil Type	ρ_{dry} °C.m/w	ρ_{wet} °C.m/w	$\nu=\rho_{dry}/\rho_{wet}$	θ_x	pf	Maximum Current Carrying Capacity			
						11kV		33kV	
						without dry band	with dry band	without dry band	with dry band
Lime	2.35	0.941	2.497	62	∞	352	299	745	690
	1.8	0.85	2.11	56	2	362	327	767	690
	1.7	0.76	2.23	58	1	372	314	791	721
25% Lime + 75% Sand	1.304	0.522	2.498	62	∞	403	321	867	710
	1.22	0.50	2.44	60	2	407	323	875	716
	1.02	0.48	2.125	58	1	410	335	882	738
Clay	1.586	0.627	2.53	60	∞	388	315	831	693
	1.53	0.61	2.5	58	2	391	316	836	696
	1.51	0.61	2.475	58	1	391	317	836	698
Sand	2.036	0.968	2.097	62	∞	350	305	738	685
	1.7	0.75	2.26	56	2	373	314	793	715
	1.46	0.75	1.95	58	1	373	322	793	727
Clay + Silt + Sand	1.69	0.83	2.036	60	∞	364	314	772	712
	1.6	0.756	1.65	58	2	372	317	792	723
	1.469	0.705	1.946	64	1	378	321	806	700
Silt + Sand	1.9	0.756	2.375	56	∞	372	336	792	712
	1.68	0.66	2.15	54	2	384	313	820	730
	1.5	0.67	2.2388	60	1	483	319	817	699

Where H is the heat conductivities matrix, θ is a vector of temperatures at the finite element mesh nodes and b, is a vector which normally contains all the heat generations associated with all nodes. Both the matrix H and the vector b are adjusted to accommodate the boundary conditions of the thermal circuit [15-19]. In this case study the soil surface (upper side in fig. 9) is represented as an isothermal boundary at ambient temperature and is described by the following equation:

$$\theta = \theta_a \quad (6)$$

Where θ_a is the ambient temperature °C. The other three sides have boundaries that are subjected to specified heat flux conditions, i.e. for each boundary side of them the divergence of the heat flux in the direction normal to the boundary side is equal to zero, and is described by the following equation:

$$\frac{\partial\theta}{\partial n} = 0 \quad (7)$$

Where n is an outward normal direction to the surface of the boundary side. Fig. 12 gives the temperature distribution around three core cable (11-kV), as a case study. The cable is loaded by 352Amp and directly buried in lime at 0.8m depth that yield the conductor maximum temperature is fixed at 90 °C. As it is concluded from the experimental results, the dry band can be formed at a critical temperature of 62°C for lime with pf=∞, as it is indicated in Table 3. Hence by drawing the isothermal contour at this critical temperature (in our case study 62°C), the shape of the dry band can be detected, which is presented by the area around the three core cable and is closed by isothermal contour at this critical temperature, as it is shown in Fig. 13.

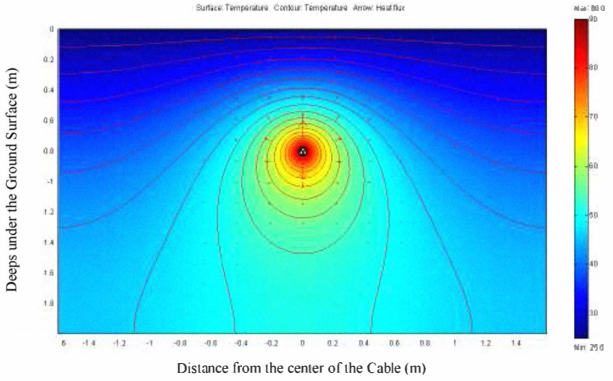

Figure 12. Temperature distribution within and around three core cable (11kV), directly buried in lime.

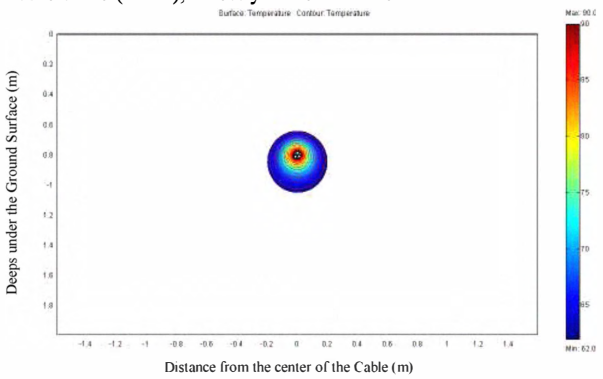

Figure 13. Dry band formation around three core cable (11kV), directly buried in lime.

CONCLUSION

From the so many tests carried out on artificial and natural soils and calculations carried out according to IEC it is found that:

1-The discontinuity in temperature-distance curve indicates the separation between the dry band and wet band and this depends on the soil type and suction tension. This means that the dry band is formed in some soils faster than the others.

2-To minimize the effect of dry band formation backfill material contains 75% sand + 25% lime can be used because it has low thermal resistivities for all pf values, and higher values of maximum current capacity can be obtained

3-The maximum current carrying capacity of under-ground power cables varies with the change of suction tension

REFERENCES

[1] IEC publication 60287-1-3, "Calculations of the continuous current rating of cables (100% load factor)", 1982.

[2] J. Hegyi and A. Klestoff, "Current-Carrying Capability for Industrial Under-ground Cable Installations", IEEE. Transactions on Industry Applications, Vol. 24, No.1 January-February 1988, pp.99-105.

[3] M.A. Hanna, A.Y. Chikhani and M.M.A. Salama, "Thermal Analysis of Power Cables in Multi-Layered Soil", Part 3: Case of Two Cables in a Trench, IEEE Transactions on Power Delivery, Vol. 9, No. 1, January 1994, pp. 572-578.

[4] G. J. Anders, H. S. Radhakrishna, "Power Cable Thermal Analysis with Consideration of Heat and Moisture Transfer in the Soil", IEEE Transactions on Power Delivery, Vol. 3, No. 4, October 1988, pp. 1280-1288.

[5] G. J. Anders, A.K.T. Napieralski, and W. Zamojski, "Calculation of the Internal Thermal Resistance and Ampacity of 3-Core Unscreened Cables with Fillers", IEEE Transactions on Power Delivery, Vol. 13, No. 3, July 1998, pp.-699-705.

[6] Koopmans G., Gouda O.E., "Transport of heat and moisture in soils with hysteretic moisture potential", 4th. International conference on numerical methods in thermal problems. 15-18 July 1985, Swansea, U.K.

[7] Gouda O.E., "Formation of the dried out zone around under-ground cables loaded by peak loadings", Modeling, Simulation & Control, ASME Press, vol. 7, No. 3, 1986, pp. 35-46

[8] Francisco de León, and George J. Anders, "Effects of Backfilling on Cable Ampacity Analyzed With the Finite Element Method", IEEE Transactions on Power Delivery, Vol. 23,No. 2, April. 2008, pp. 537-543.

[9] Ossama E. Gouda, Adel Z. El Dein and Ghada M. Amer, "Effect of dry zone formation around underground power cables on their ratings", International Journal of Emerging Electric Power Systems: Vol. 10 : Issue 2, Article 1. 2009

[10] G. J.Anders, M. Chaaban, N. Bedard and R.WD. Ganton, "New Approach to Ampacity Evaluation of Cables in Ducts Using Finite Element Technique", IEEE Transactions on Power Delivery, Vol. PWRD-2, No. 4, October 1987, pp. 969-975.

[11] F. Donazzi, E. Occhini and A. Seppi, "Soil thermal and hydrological characteristics in designing under-ground cables", Proc. IEE, Vol. 126, No. 6, June 1979.

[12] Hartley, J.G., Black, W.Z., "Transient Simultaneous Heat and Mass Transfer in Moist Unsaturated Soils", ASME Trans., Vol. 103, May 1981, pp.376-382.

[13] Anders, "Rating of Electric Power Cables", IEEE Press/McGraw-Hill 1998.

[14] Neher, J.H., McGrath, M.H., "The Calculation of The Temperature Rise and Load Capability of Cable Systems", AIEE Trans., Vol. 76, Pt. 3, October 1957, pp. 752-772.

[15] M.A. El-Kady, Ontario Hydro, "Calculation of the Sensitivity of Power Cable Ampacity to Variations of Design and Environmental Parameters", IEEE Transaction on Power Apparatus and Systems, Vol. PAS-103, No. 8, August 1984, pp. 2043-2050.

[16] Carlos Garrido, Antonio F. Otero, and José Cidrás, "Theoretical Model to Calculate Steady-State and Transient Ampacity and Temperature in Buried Cables", IEEE Transactions on Power Delivery, Vol. 18, No. 3, July 2003, pp. 667-678

[17] M. A. Kellow, "A Numerical Procedure for the Calculation of the Temperature rise and Apacity of Under-ground Cables", IEEE Transactions on Power Apparatus and Systems, Vol. PAS-100, No. 7 July 1981, pp. 3322-3330

[18] O. T. Hassan, "Effect of Dry Zones Formation on the Insulation Life Time of Under-ground Cables", M.Sc. Cairo University , Faculty of Engineering, April 1999.

[19] M.A. Mahmoud, "De-Rating Factor of Under-ground Power Cables Ampacity Due to Dry Zone Formation", M.Sc. Cairo University, Faculty of Engineering, 2009.